Geological Society, London, Special Publications

$^{40}Ar/^{39}Ar$ geochronology and the diffusion of ^{39}Ar in phengite–muscovite intergrowths during step-heating experiments *in vacuo*

Marnie A. Forster and Gordon S. Lister

Geological Society, London, Special Publications 2014, v.378; p117-135.
doi: 10.1144/SP378.16

Notes

$^{40}Ar/^{39}Ar$ geochronology and the diffusion of ^{39}Ar in phengite–muscovite intergrowths during step-heating experiments *in vacuo*

MARNIE A. FORSTER* & GORDON S. LISTER

Research School of Earth Sciences, Australian National University, Canberra, ACT 0200, Australia

**Corresponding author (e-mail: marnie.forster@anu.edu.au)*

Abstract: Step-heating experiments *in vacuo* are routine when conducting $^{40}Ar/^{39}Ar$ geochronology, including for white mica. White mica can break down, due to dehydroxylation and delamination, so experiments involving mica are often conducted in relative haste, and not with the care and precision necessary when intending to apply multi-diffusion-domain theory to model the results. Here we show, however, that carefully managed step-heating experiments appear to allow release of argon through solid-state diffusion processes alone. We analysed phengite-muscovite intergrowths in high-pressure metamorphic rocks exhumed in and beneath extensional ductile shear zones during continental extension. Such materials often yield Arrhenius plots in which there is a distinct steepening of slope mid-way through the step-heating sequence. This steepening appears to correspond with steps in which release of argon from phengite components dominate. We analysed the data using a computer program (*eArgon*) and numerically simulated mixing of gas released from multiple diffusion domains. The results suggest that diffusion of ^{39}Ar in phengitic white mica involves radically different diffusion parameters in comparison with muscovite. If these results extrapolate to nature then $^{40}Ar/^{39}Ar$ geochronology may allow direct dating of white mica mineral growth during metamorphism.

Supplementary material: Data files A, B and C are available at www.geolsoc.org.uk/SUP18619.
Data file A C++ computer code used to infer data for an Arrhenius plot, assuming different diffusion geometries. These methods are excerpted from the *eArgon* computer program used to analyse these data.
Data file B Analytical methods and procedures used in the laboratory for $^{40}Ar/^{39}Ar$ geochronology performed on the samples reported.
Data file C XML formatted data tables for the step-heating experiments reported in this study, in a form that can be read by the *eArgon* computer program.

Step-heating experiments are routinely conducted for the purposes of $^{40}Ar/^{39}Ar$ geochronology, but only rarely has diffusional modelling been undertaken in an effort to extract information from white mica as to the duration of heating events or as to the nature of the pressure–temperature–time path to which the minerals were subjected in the natural environment (Wijbrans & McDougall 1986, 1988; Hames & Bowring 1994; Kirschner *et al.* 1996; Lister & Baldwin 1996; Lister & Raouzaios 1996; Baldwin & Lister 1998; Forster & Lister 2004; Mulch *et al.* 2005; Harrison *et al.* 2009; Kula *et al.* 2010; Forster *et al.* 2011; Viete *et al.* 2011). This is because, for the last few decades, the consensus has been that hydrous minerals break down *in vacuo* (e.g. McDougall & Harrison 1999).

Fortunately, it now appears that this is not always the case (Harrison *et al.* 2009; Forster *et al.* 2011; Kula & Spell 2012) and solid-state diffusion during step-heating experiments may be pertinent to a wider range of minerals than has so far been assumed. There is, perhaps, some justification for the same careful step-heating experiments with white micas as are conducted with K-feldspar in order to perform multi-diffusion domain (MDD) analysis (Lovera *et al.* 1997, 2002). MDD analysis attempts to infer the history of temperature with time followed by individual samples in the natural environment, and is therefore a useful geochronological tool. MDD methods do suffer some fundamental deficiencies (e.g. the assumption that the present microstructure has always been present, implying that it evolved without modification). Nevertheless, provided these aspects can be addressed at least in part, MDD methods offer valuable constraint, and it would be extremely useful if MDD methods could be adopted in respect to the analysis of the pattern of gas release observed for common fabric-forming minerals such as white mica.

From: JOURDAN, F., MARK, D. F. & VERATI, C. (eds) 2014. *Advances in $^{40}Ar/^{39}Ar$ Dating: from Archaeology to Planetary Sciences*. Geological Society, London, Special Publications, **378**, 117–135.
First published online July 25, 2013, http://dx.doi.org/10.1144/SP378.16

There has thus been increased interest in the diffusion of argon in white mica as more data emerge that support the hypothesis that solid-state diffusion is responsible for the release of argon during step-heating experiments *in vacuo* during $^{40}Ar/^{39}Ar$ geochronology (Sletten & Onstott 1998; Forster & Lister 2004; Harrison *et al.* 2009; Cosca *et al.* 2011; Forster *et al.* 2011; Kula & Spell 2012). It would be interesting if this is true, for then geochronologists could thereby more readily extract information as to the heating and cooling path followed by rocks in nature (e.g. Viete *et al.* 2011). However, it may be that subtle variations in mineral chemistry and/or gross differences in experimental method preclude this outcome (Forster & Lister 2004); for example, by enhancing breakdown (including delamination, dehydroxylation or as yet unspecified metamorphic reactions). Nevertheless, we contend that, in many cases, solid-state diffusion appears to govern the release of ^{39}Ar from phengitic white mica, and useful data can be extracted in particular if the schedule of heating steps is carefully managed.

Forster *et al.* (2011) reported a step-heating experiment conducted using white mica that was first irradiated and then heated at relatively low temperatures in order to expel extraneous argon. The Arrhenius data was then analysed using the same Fundamental Asymmetry Principle recognized for fractal grain size–domain volume relationships in K-feldspar (Forster & Lister 2010). The results indicate that such experiments can estimate values for critical diffusion parameters similar to those measured in carefully controlled experiments on mica reported by Harrison *et al.* (2009), which were conducted within its stability field, and under pressures of 10 and 20 kbar. However, to achieve this result, step-heating experiments with white mica *in vacuo* had to be carefully controlled in terms of temperature and the sequence of heating steps. In addition, prior to beginning the experiment, volatiles including extraneous argon needed to have been degassed from high-diffusivity pathways by heating the sample for a long period at relatively low temperatures before the experiment commenced (Forster *et al.* 2011).

In this paper we continue development of this topic by examining the results of step-heating experiments conducted on phengite–muscovite intergrowths in high-pressure rocks. Intergrowth of phengitic white mica with muscovite is typical of many high-pressure rocks (Fig. 1), principally because such rocks must be exhumed for us to see them, and their uplift from depth usually takes place as the operation of ductile shear zones in which white mica continues to grow. The shear zones provide a pathway that allows the introduction of water into the rock mass, and, in consequence, microstructures show the impact of deformation and fluid-enhanced metamorphic alteration, crystallization and/or recrystallization. Compositional variation reflects pressure and temperature conditions, and mineral chemistry typically reflects depressurization, thereby leading to complex fine intergrowths of phengitic white mica and muscovite. An ability to extract ages from different elements of such microstructure is thus important and a prerequisite if $^{40}Ar/^{39}Ar$ geochronology is to provide information that is useful in helping to constrain the duration and timing of the tectonic processes that take place during the formation and the subsequent exhumation of such terranes.

Detail as to what might constitute an ideal step-heating schedule does vary from sample to sample, and trial and error is occasionally the only way to develop a foretaste of what might be expected. It is particularly important to choose heating schedules that avoid large percentages of gas released in one heating step, for example. Often, however, it is a question of continuously monitoring the pattern of gas release and adjusting the schedules accordingly.

It is possible to obscure information that would otherwise be available in an apparent age spectrum; for example, if a step-heating experiment is started at too high a temperature (e.g. Kula *et al.* 2010), thereby ensuring chaotic mixing. It is also possible to obtain confusing data if sufficient 'cleaning' time is not allowed in order that a sample loses 'volatiles' from high-diffusivity pathways before the step-heating experiment is commenced. In general, such 'cleaning' time ensures the release of 'extraneous' argon and minimizes (or eliminates) the effect of 'excess argon' in the initial steps (cf. Sherlock *et al.* 1999). We would suggest that the use of a laser in such circumstances should be deprecated. Similarly, data from $^{40}Ar/^{39}Ar$ geochronology should not be so readily set aside based on *a priori* assumptions as to the 'relevant' closure temperature (cf. Sherlock & Arnaud 1999). In this aspect we also note that it is our experience that Rb–Sr offers an unreliable and readily reset geochronometer that typically reflects the timing of the last period of fluid activity in the deforming rock mass, and cannot be used to provide quality control for $^{40}Ar/^{39}Ar$ geochronological data.

In particular, the work we present here is of interest because mixtures of phengitic white mica with muscovite have been thought to behave in a manner that is incompatible with the diffusion hypothesis (Wijbrans & McDougall 1986, 1988; Kula *et al.* 2010). The apparent age spectra imply that argon is released, first from muscovite, then phengite and then back to muscovite again, producing characteristic 'hump-backs' in the apparent age

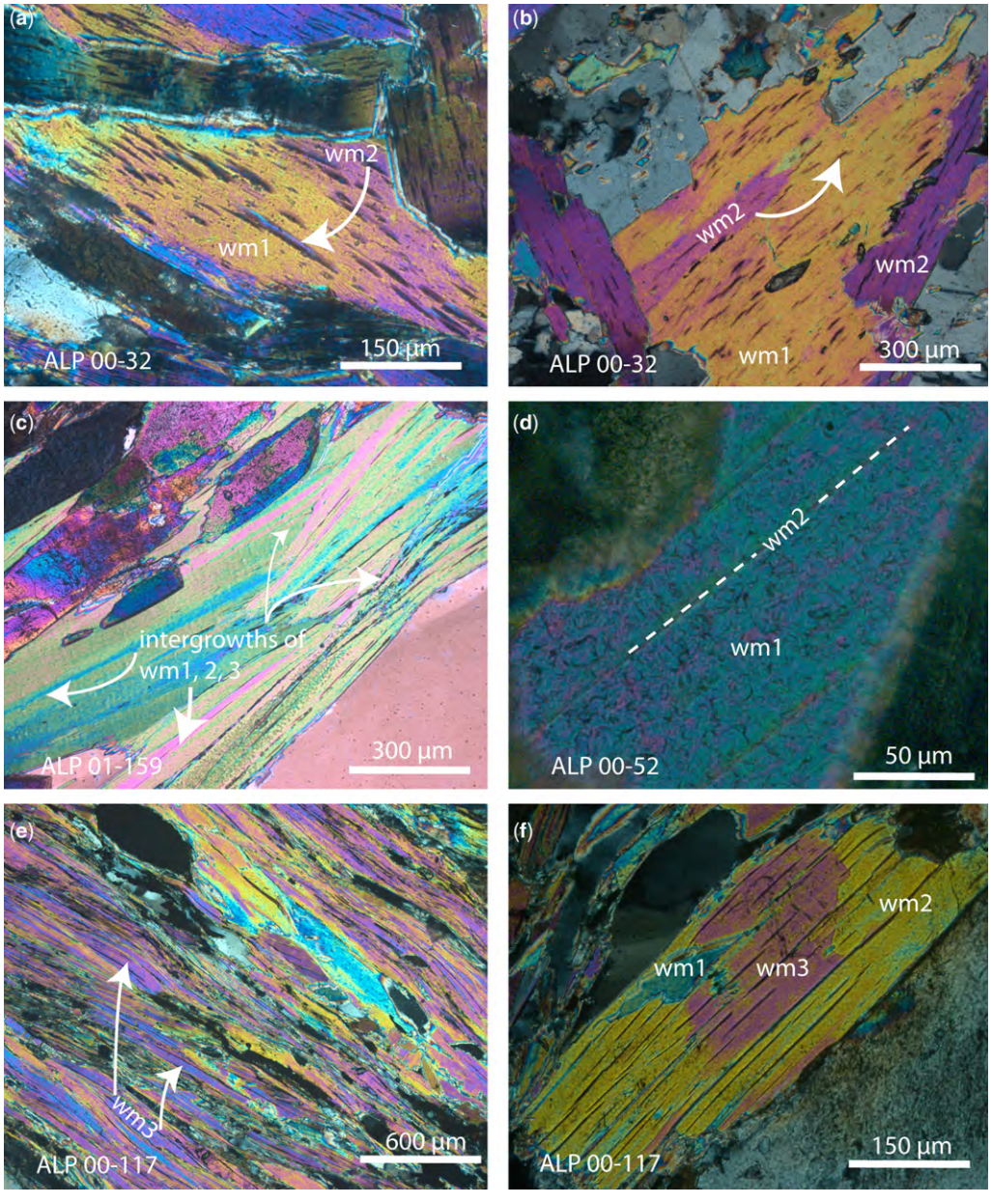

Fig. 1. Microstructures show different types of intergrowths between different generations of muscovite and phengitic white mica: (**a**) shows two different microchemical zones, with younger overprinting growth within larger grains, in ALP00-32; (**b**) decussate recrystallization of a younger generation of white mica grown, in ALP00-32; (**c**) complex intergrowth of white mica along cleavage planes in ALP01-159, with three different generations recognizable; (**d**) intergrowths along cleavage planes in ALP00-52; (**e**) elongate grains from a phyllonitized button-schist in the Entrelor Shear Zone, ALP00-117; and (**f**) larger grains in ALP00-117 were not analysed but they show three generations of white mica. Sample locations are given in Table 1.

release spectra (Fig. 2). Spectra such as this (where steps with older apparent ages are followed by steps in which younger ages are measured) do seem to provide evidence that processes other than diffusion are at work, since it seems at first sight that this phenomenon could not be explained by progressive

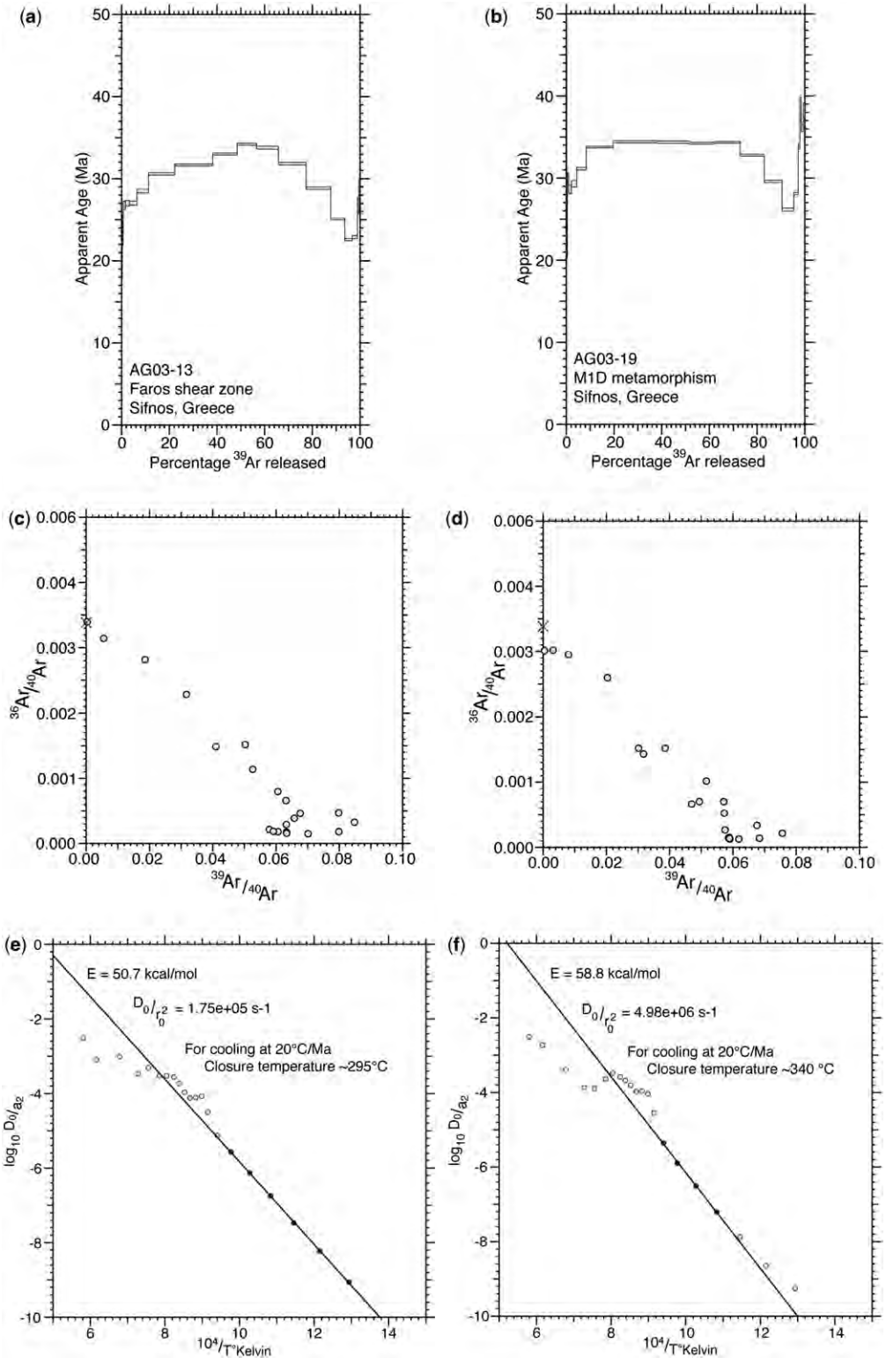

Table 1. *Location data for samples discussed in this paper*

Sample locations	Latitude	Longitude	Unit	Place	Country
ALP00-32	45°24.447′N	7°31.750′E	Sesia Zone	Sparone	Italy
ALP00-52	45°32.903′N	7°43.877′E	Sesia Zone	Cime de Bonze	Italy
ALP00-117	45°32.874′N	7°9.464′E	Entrelor Shear Zone	Col de l'Entrelor	Italy
ALP01-159	45°52.722′N	7°35.492′E	Zermatt–Saas ophiolite	Lago di Cignana	Italy
AG03-13	36°56.357′N	24°45.291′E	Faros shear zone	Sifnos	Greece
AG03-19	36°59.709′N	24°42.476′E	M1D type locality	Sifnos	Greece

degassing as the result of solid-state diffusion. Gas release in these higher temperature parts of a step-heating sequence are usually attributed to delamination, dehydroxylation or to as yet undetermined metamorphic breakdown reactions (Forster & Lister 2004). However, in this paper we show that this assumption may be incorrect, and demonstrate that (at least for phengite–mica intergrowths) such behaviour (where a succession of older steps is followed by a succession of younger steps) can be a naturally emergent property of a mixture of minerals with widely differing frequency factors.

Table 1 provides location data for the samples reported in this study. It should be noted that there are many more samples than those listed that display the phenomena discussed here. The samples chosen have been selected on the basis of the morphological variety of apparent age spectra that can thereby be included.

Arrhenius data from phengite–muscovite intergrowths

Experiments on mixtures of muscovite and phengitic white micas were first conducted by Wijbrans & McDougall (1986, 1988). They showed that younger ages from muscovite first become evident in the apparent age plot because, initially, gas is preferentially released from less retentive microstructural reservoirs. Thereafter, release of gas from phengite dominates the age produced by the individual steps, which to date has been an inexplicable observation. Prior to undertaking this work we had assumed that, during the step-heating experiment, the material was heated to sufficient temperature that the release of gas occurred during dehydroxylation and delamination, or even as the result of metamorphic recrystallization or partial melting in the furnace. We have no direct information as to the nature of these processes, however.

As mentioned above, step-heating experiments *in vacuo* are routinely conducted for the purposes of $^{40}Ar/^{39}Ar$ geochronology (McDougall & Harrison 1999). Diffusion data can potentially be extracted from such experiments because ^{39}Ar is not produced in nature but during the course of irradiation in a nuclear reactor, prior to the actual step-heating experiment being performed. If it is assumed that the concentration of ^{39}Ar is initially uniform within a diffusion domain, the percentage release of ^{39}Ar can be analysed in terms of well-known equations (Crank 1975; McDougall & Harrison 1999; Watson *et al.* 2010) to extract D/a^2 for each heating step, where D is the frequency factor and a is the diffusion radius.

Our results show that the shape of Arrhenius plots obtained during experiments on phengite–muscovite intergrowths often show characteristic (and sometimes abrupt) increases in slope as the temperature of the heating step increases. We were able to show that such changes are explicitly associated with 'hump-backed' spectra (as illustrated in Fig. 2), but also that the phenomenon is of much more general occurrence in high-pressure rocks (as illustrated in Fig. 3). Some aspects of these curves can be the result of fractal feathering of diffusion domains (Forster *et al.* 2011) but, since such effects are usually limited to the first few steps of gas release, this cannot be the full explanation. An alternative hypothesis might be that such variation is the result of anisotropic diffusion (Huber *et al.*

Fig. 2. 'Hump-backed' apparent age spectra are typical of step-heating experiments conducted on complex intergrowths of muscovite and phengite from exhumed high-pressure metamorphic rocks. The examples are from the M1D tectonic slice on Sifnos, Cyclades, Greece: (**a**) & (**b**) apparent age spectra from AG03-13 and AG03-19 show the effect of an increased percentage of muscovite in the overprinting shear zone at the base of the slice; (**c**) & (**d**) the York plots show progressive degassing during the early stages of the step-heating experiment, dominated by release from muscovite; (**e**) & (**f**) Arrhenius data showing diffusion parameters estimated for the muscovite component taking no account of the effect of mixing. Note that the steepening of the slope is typical of the presence of phengite in these samples.

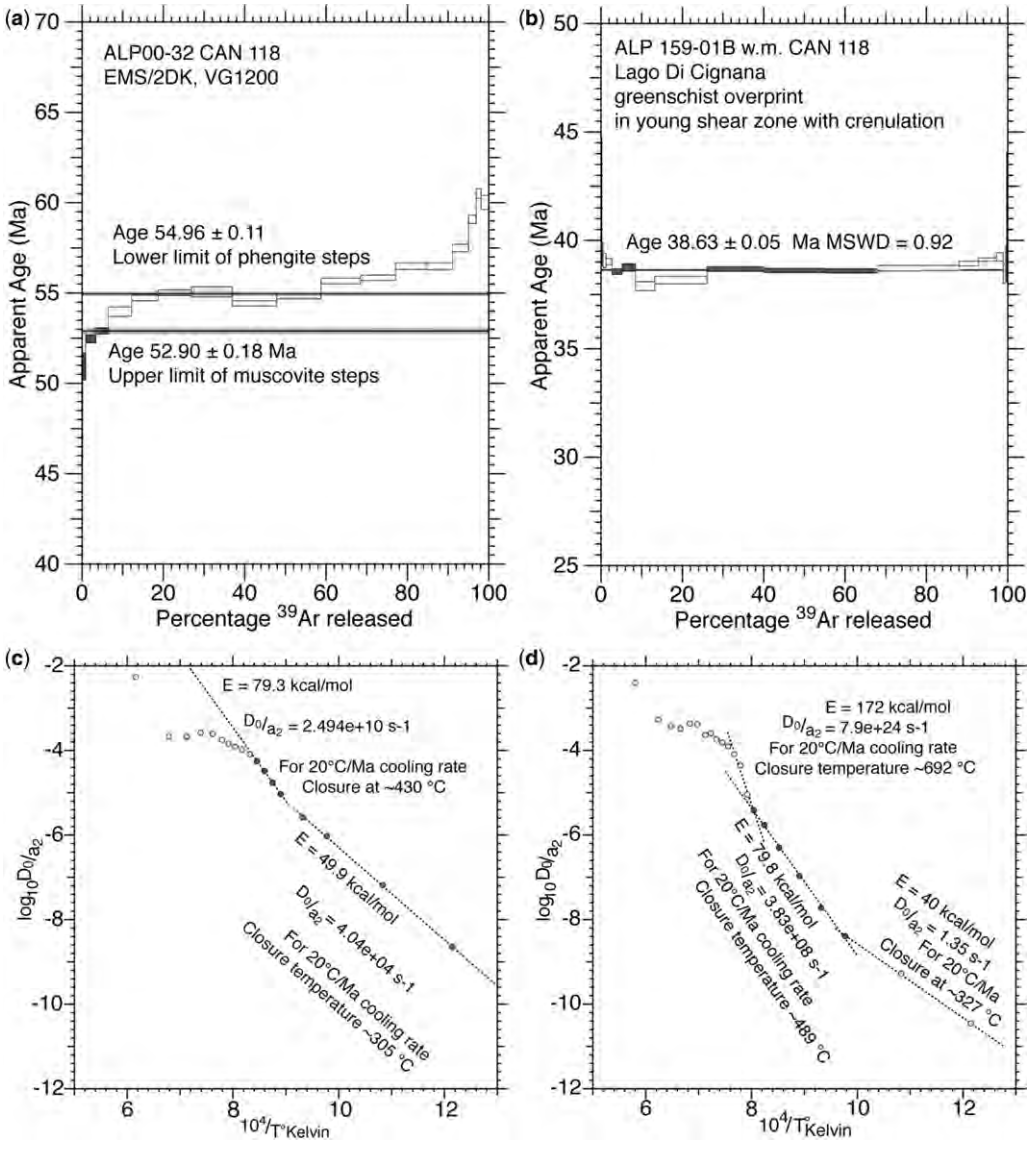

Fig. 3. Apparent age spectra from muscovite–phengite mixtures (**a**) & (**b**) do not always develop a 'hump-backed' form. The presence of phengite is, however, typified by the changes of slope evident in the Arrhenius plots (**c**) & (**d**).

2011) with temperature-dependent diffusion parameters. Thereby, as temperature increases, different diffusion constants apply. Huber *et al.* (2011) used a three-dimensional (3D) Boltzmann model to obtain gradual changes of slope that are reminiscent of some natural data.

There is a third hypothesis, however. These strangely shaped Arrhenius plots can be quantitatively explained by the mixing of gas released from white mica with different crystal chemistry and, perhaps, vastly different diffusion parameters. As noted above, the progressive release of ^{39}Ar during a step-heating experiment allows an estimate to be made as to the diffusion parameters that applied during the experiment. However, the numbers that are obtained depend on the assumptions made, in particular in respect to geometry. In terms of the numerical analysis, for limited time ranges it is not important what geometry is chosen for this exercise. But once that decision has

been made it should be realized that the different parameters are not interchangeable. For example, Warren *et al.* (2011) made the mistake of using parameters estimated by Harrison *et al.* (2009) based on a spherical geometry to perform calculations that assumed a cylindrical geometry. Thereby, the details of their calculations are invalidated. This is not important if one is concerned only with principles, but note these had already been expostulated (Lister & Baldwin 1996). The factors that affect diffusion parameters are manifold. No single variable determines the outcome of a diffusion experiment. We must consider geometry, activation energy, activation volume and frequency factor as a coupled parameter set.

Extracting diffusion data from experiments

These points are illustrated by analysis of data obtained from muscovite in a button-schist from the Entrelor Shear Zone in the Western Alps (see Table 1 for the sample and location details).

Figure 4 shows the apparent age plot and associated Arrhenius data. The key observation is that if we change the slope of a line drawn through a cluster of Arrhenius data points, the inferred frequency factor and the inferred activation energy must vary in tandem.

Table 2 shows the analysis of these data using different initial diffusion geometries. While there is usually relatively little variation in the estimated activation energy, this is not so for estimates as to the frequency factor and the effective diffusion distance, however. These data are produced by numerical analysis of particular datasets, and the diffusion parameters that are obtained are intrinsically dependent on the assumption made as to the geometry of the diffusion domains involved: including factors such as 'roughness' as approximated using fractals by Forster & Lister (2010); or different 3D geometries analysed using a Boltzmann model (Huber *et al.* 2011); or using the 3D (second-rank) diffusion tensor (Watson *et al.* 2010). The geometry assumed for analysis may change the derived parameters by approximately 30%, in the case of the activation energy that will be estimated, or by orders of magnitude in the case of the normalized frequency factor (i.e. D_0/a^2).

Data from the sample from the Entrelor Shear Zone allow estimates as to the closure temperature for muscovite (for cooling at a rate of 20 °C/Ma) that is not different from the oft quoted value of 350 °C 'generally assumed for moderate cooling rates' (McDougall & Harrison 1999, p. 26). We emphasize that this is so, however, only because we chose an example that made this to be the case. Closure temperature depends on the cooling rate and the assumed ambient pressure (as illustrated by Lister & Baldwin 1996). There is no single 'closure temperature' that should be quoted as characteristic of a particular mineral.

The reader should note that analysis of the Entrelor sample provides an estimate for the activation energy (*c*. 67 kcal/mol) that is 10–12% higher than the values obtained by analysis of experimental data (Giletti 1974; Giletti & Tullis 1977; Harrison *et al.* 2009). Any increase in retentivity is offset by the relatively high values obtained for the frequency factor, however. This is because the frequency factor can be translated loosely in non-mathematical terms as the maximum diffusivity that could ever be measured and, as evident from the diffusion equation, higher frequency factors narrow the range during which a mineral grain will rapidly degas. It should be emphasized that there is considerable variation in the parameters that can be estimated in this way and, therefore, claims that results from step-heating experiments *in vacuo* which mimic experimental data (e.g. Harrison *et al*. 2009; Kula & Spell 2012) should be treated with caution. The range of diffusion parameters that apply in nature may be far greater than presently published experimental data would allow.

Modelling mixing

Although the Arrhenius data from the Entrelor sample (Fig. 4) may be correctly taken to imply that the material measured was dominantly muscovite, inferences based on Arrhenius data that display changes in slope (Figs 2 & 3) are inherently more difficult. Here, below, we focus on that aspect of the problem, detailing results of modelling and simulation of Arrhenius data that result from mixing. We will document detailed data as to the microchemistry and tectonic evolution of these rocks in a later publication.

Our simulations demonstrate that variations in diffusion parameters allow quantitative explanations of data obtained from step-heating experiments on mixtures of phengite and muscovite. We can at least in part substantially replicate data produced from the mass spectrometer, at least for the bulk of the experimental data. We have not focused on temperature steps above 1200 °C because we are uncertain as to whether metamorphic breakdown reactions have commenced by that time.

Our results imply that phengite and muscovite have vastly different diffusion parameters, supporting the hypothesis (Wijbrans & McDougall 1986, 1988; Lister & Baldwin 1996) that phengitic white mica is at least initially more retentive than muscovite in terms of argon diffusion. To our surprise,

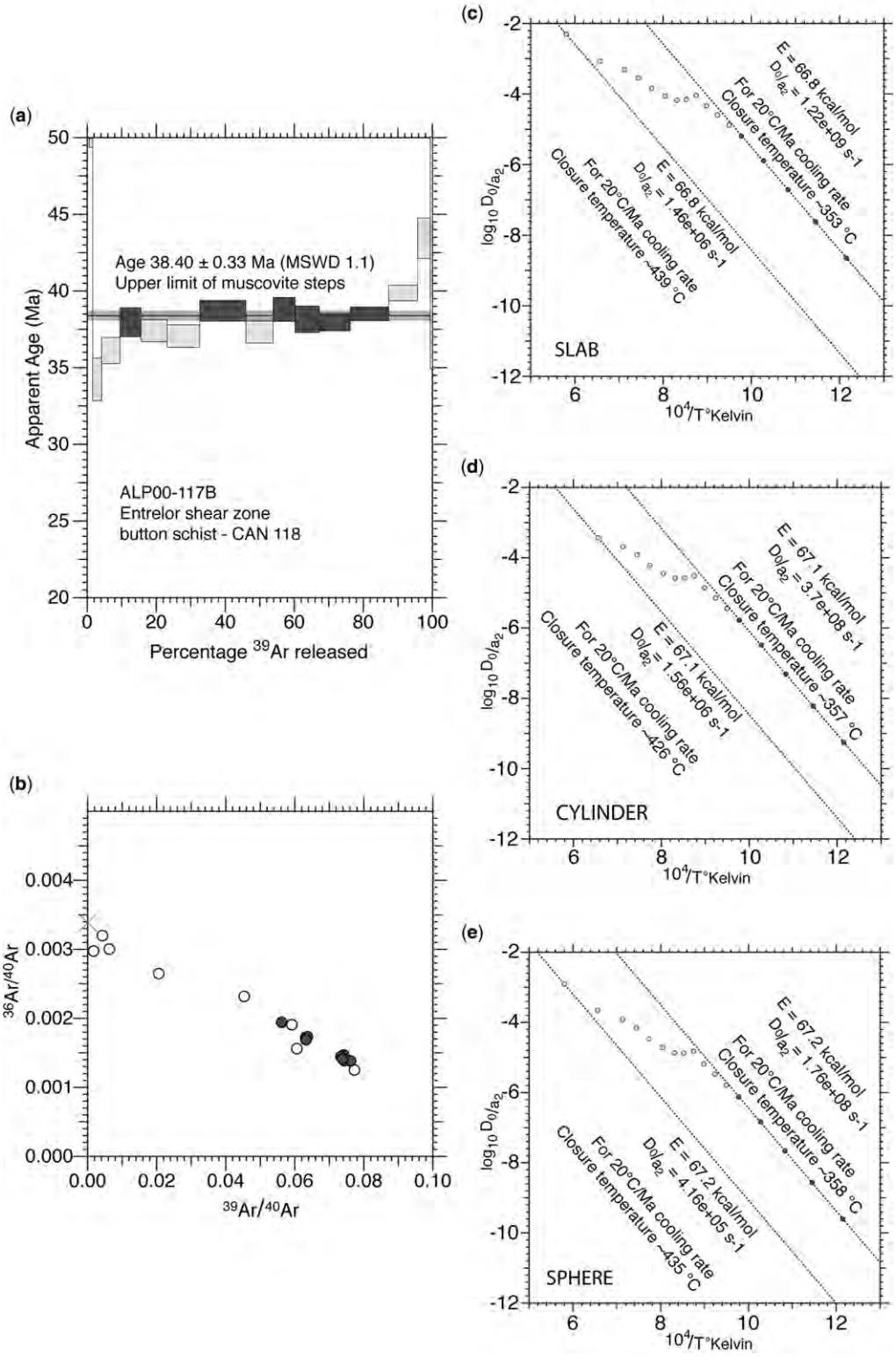

Table 2. *Diffusion data estimated for muscovite in ALP00-117 using different assumptions as to the initial diffusion geometry*

Assumed geometry	Activation energy (kcal/mol)	D_0/a^2 (s^{-1})	Closure temperature for cooling at 20 °C/Ma (°C)	Frequency factor ($cm^2\ s^{-1}$)	Diffusion radius (μm)
Slab	66.8	1.22×10^9	353	4.0	0.57
Cylinder	67.1	3.71×10^8	357	4.0	1.04
Sphere	67.2	1.76×10^8	358	4.0	1.51

however, our simulations show that variations in the frequency factor mean that this circumstance is reversed at higher temperature. Since muscovite crystals were formed later in the metamorphic history, the apparent age plot thus initially rises in age and then falls, producing the 'hump-backed' spectra (Fig. 2) that are typical of such mixtures (Wijbrans & McDougall 1986).

In this section we first present simulations that show how this pattern of gas release may be the outcome of the vastly different diffusion parameters. Orders of magnitude relative increases in frequency factor mean that phengite is retentive but, once degassing becomes significant, the argon is released over a relatively narrow temperature range (Fig. 5). Depending on relativity, circumstances may apply that ensure that once the more retentive phengite reservoirs have been exhausted, the release of gas from the muscovite domains again becomes evident.

We forward model the release of ^{39}Ar from a mixture of phengitic white mica and muscovite quite simply, using the formulae ensconced in the *C++* program code provided in the supplementary material. The diffusion parameters for our model muscovite are held constant (see Fig. 5) while, for our model phengite, the frequency factor is systematically varied over several orders of magnitude. Arrhenius plots (Fig. 6a–f) show the variation that may be expected due to the variation in the assumed frequency factor, while Figure 5 shows the relative percentages of gas released during heating steps at different temperatures during these simulations.

The lesson that can be drawn from Figure 5 is that the relative percentage of gas release from phengite v. muscovite depends critically upon the frequency factor. Although the activation energy for phengite assumed in these simulations is double that assumed for muscovite, it is the frequency factor that determines whether gas release from phengite is subsequent to the degassing of muscovite (Fig. 6a, b), or coeval (Fig. 6c, d), or something else. For a wide range of frequency factor values, phengite releases argon over relatively narrow temperature ranges, in a burst, while muscovite degassing continues (more slowly) before and after (Fig. 6e, f). In this frequency factor range, phengite degassing overwhelms the release of ^{39}Ar from model muscovite only after this mineral has already degassed significantly. As the temperature rises, phengite degassing is exhausted, at which time the release of gas from the model muscovite begins once again to dominate.

This is an unexpected result, although it should not have been as mathematically it is obvious. The diffusion of argon in white mica can be estimated using the Arrhenius Law to calculate diffusivity. The diffusivity (D) can be related to a frequency factor (D_0) and an activation energy (Q):

$$D = D_0 \exp(-Q/RT) \quad (1)$$

where R is the gas constant and T is the absolute temperature. The activation energy itself is determined by the value at zero pressure (E) and a pressure correction to take account of the reduced diffusivity that ensues as pressure increases. Hence, the activation energy is usually presented as:

$$Q = E + P\bar{v} \quad (2)$$

where $\bar{v}$ is the activation volume and P is the pressure (in this case in kbar). Using this equation implies that diffusivity is dependent on both the

Fig. 4. An apparent age plot (**a**) and corresponding York plot (**b**) from muscovite in a button-schist from the Entrelor Shear Zone in the Western Alps. Inference as to the diffusion parameters can be made using the Arrhenius data, but different answers (Table 2) are obtained depending on the assumed geometry (**c**)–(**e**). Note that under exceptional circumstances a York plot allows recognition of an 'inverse isochron'. However, since this is rarely the case, referring to such plots as 'Inverse Isochron Diagrams' is not appropriate, in particular when dealing with samples that do not display a single age variably mixed with air.

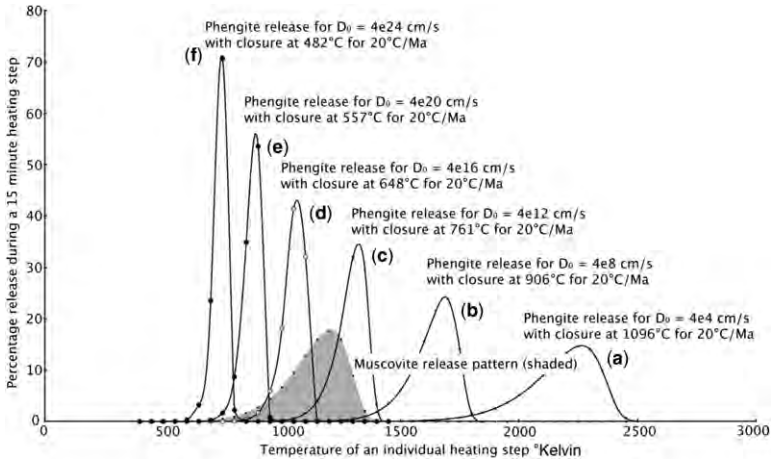

Fig. 5. Arrhenius data from a mixture of muscovite and phengite showing the effect of vastly different diffusion parameters, principally illustrating the influence of the frequency factor. In (**a**) & (**b**) as temperature increases, muscovite degasses and then the phengite. In (**c**) & (**d**) mixing occurs throughout the experiment, with muscovite degassing first (d), then to be overtaken by phengite which degasses in a burst, only to be overtaken by gas release from muscovite. In (**e**) & (**f**) phengite degasses first, and then the muscovite. See Figure 6 for the diffusion parameters utilized.

exponential and the pre-exponential constants, and one constant should not be taken into consideration without noting the effect of the other. In essence, the pre-exponential constant (i.e. the frequency factor) acts as a scaling variable, narrowing the temperature range over which the transition from zero diffusivity to maximum diffusivity will be obtained.

Inversion of Arrhenius data to allow estimation of diffusion parameters

The work reported above suggests that we should be able to 'invert' the Arrhenius data obtained from a particular step-heating experiment to obtain an estimate as to the actual diffusion parameters (in this case the activation energy and the frequency factor) that applied. Therefore the final step of our analysis was to take some real Arrhenius data and to attempt inversion by forward modelling different choices of the diffusion parameters to see how well we can match the data provided. Intergrowths of phengitic white mica and muscovite are evident in sample ALP00-52 from Cime de Bonze in the Sesia Zone, Italy, in the Western Italian Alps (Fig. 7), close to the sample analysed by Rubatto *et al.* (2011). The apparent age spectrum (Fig. 7a) and the York plot (Fig. 7b) show patterns of gas release that are typical of such mixtures, namely an asymptotic rise of apparent age, while release from muscovite dominates, allowing an estimate for the age of the initial exhumation of these high-pressure eclogites.

We performed each iteration sequence manually, using the *eArgon* program. This iterative approach can be automated, but we have not done this yet. Here we provide one example that shows how simply and how readily one can match observed data, and thus provide an estimate for the diffusion parameters for both phengite and muscovite in a mixture.

The first step in the inversion process was to estimate the diffusion parameters for the inferred muscovite part of the apparent age spectrum (Fig. 8a). This provided an estimate of diffusion parameters, as follows, assuming a spherical geometry: (a) $E = 58.22$ kcal/mol; and (b) $D_0/a^2 = 3.887 \times 10^5\ s^{-1}$. If the frequency factor is $D_0 = 4\ cm^2\ s^{-1}$, as inferred by Harrison *et al.* (2009) from their experimental data, this implies a diffusion radius of approximately 32 μm and for cooling at zero pressure, at 20 °C/Ma, a closure temperature of about 343 °C.

The next step was to estimate the diffusion parameters for the part of the spectrum dominated by

Fig. 6. A plot of phengite gas release v. muscovite for the range of frequency factors shown in Figure 5. There is a wide range of frequency factors that allow patterns of gas release as observed in nature from such mixtures. The diffusion parameters for muscovite are held constant as a matter of convenience in these simulations to allow the effect of the relative variation to be discerned.

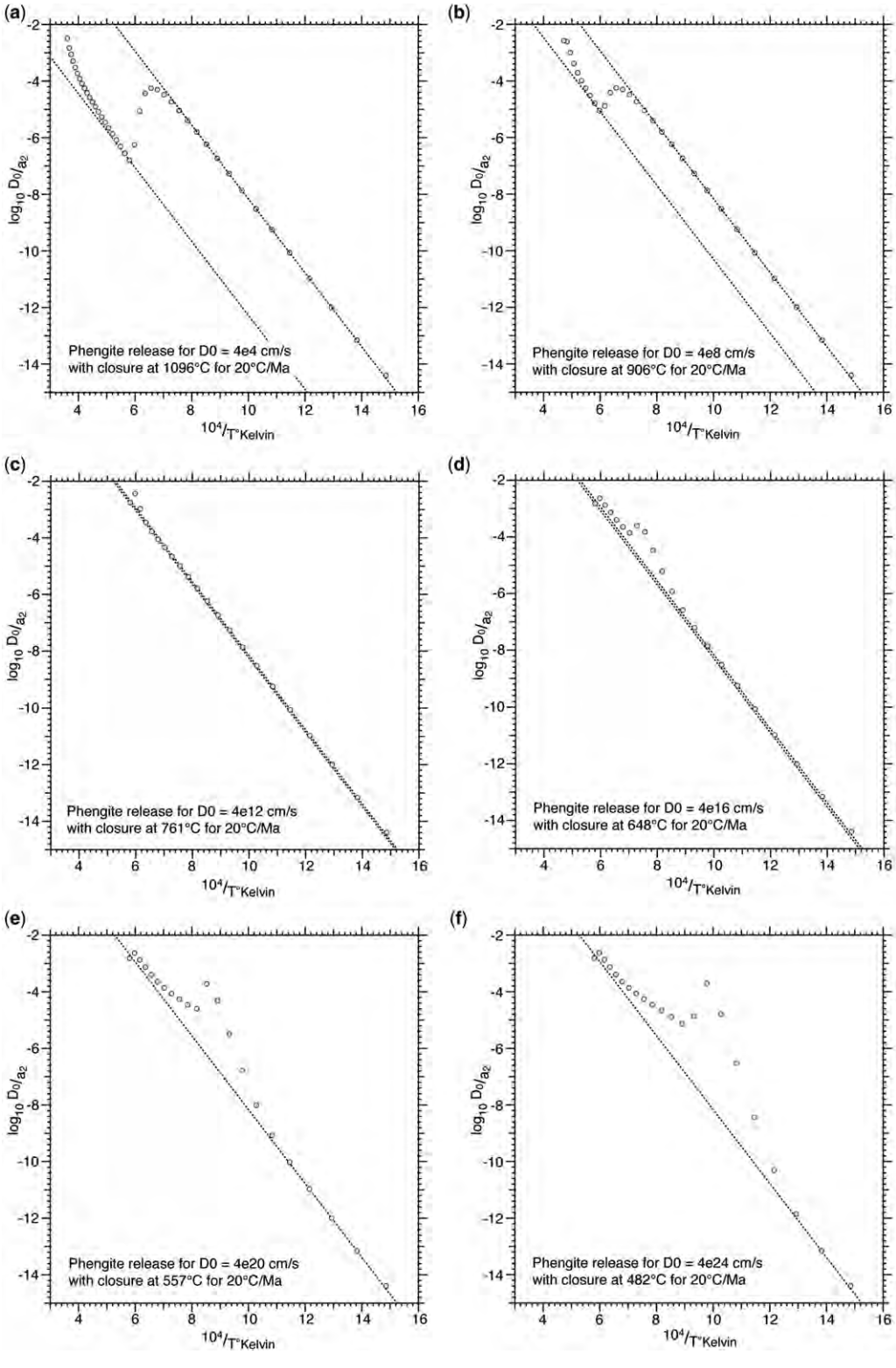

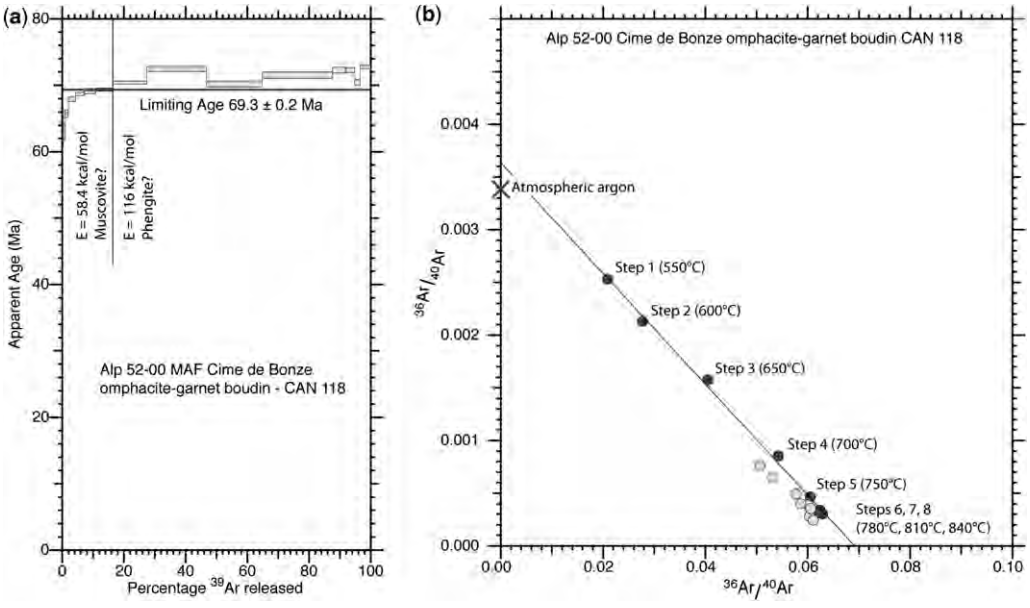

Fig. 7. Intergrowths of phengitic white mica and muscovite are evident in sample ALP00-52 from Cime de Bonze in the Sesia Zone, Italy, in the Western Italian Alps. The apparent age spectrum (**a**) and the York plot (**b**) show patterns of gas release that are typical of such mixtures, namely an asymptotic rise of apparent age while release from muscovite dominates, allowing an estimate for the age of the initial exhumation of these high-pressure eclogites.

phengite release. Here we selected the maximum value of the activation energy consistent with the Arrhenius data (Fig. 8a), noting that we have shown that this strategy will nevertheless underestimate actual model mineral diffusion parameters. The values thus chosen were: (a) $E = 168$ kcal/mol; and (b) $D_0/a^2 = 7.501 \times 10^{26}$ s^{-1}. With a frequency factor of $D_0 = 4 \times 10^{22}$ cm^2 s^{-1}, the diffusion radius would be approximately 73 μm. Such a model mineral would close at about 649 °C at a cooling rate of 20 °C/Ma.

Forward modelling (Fig. 8b) shows that these two parameter sets estimate quite well the part of the Arrhenius plot dominated by the release of ^{39}Ar from phengite, but considerably underestimate the frequency factor for muscovite. The data estimated from the slope of the phengite-dominated segment of the Arrhenius plot would be 118 kcal mol with $D_0/a^2 = 1.74 \times 10^{17}$ s^{-1}, which is comparable with the values estimated from the real data over the four steps in this segment (Fig. 8a) from which an activation energy of 121 kcal/mol can be estimated and $D_0/a^2 = 9.37 \times 10^{17}$ s^{-1}. Clearly these are values that differ substantially (by a factor of *c.* 30% in the case of the activation energy) from the model phengite values that are necessary to replicate this part of the Arrhenius plot. We then iterated the forward model to better estimate the frequency factor for the muscovite-dominated part of the release spectrum, finally changing D_0/a^2 to 1.556×10^6 s^{-1} (implying a 16 μm diffusion radius for $D_0 = 4 \times 10^{22}$ cm^2 s^{-1}).

Interestingly, and as is evident in the plots of the synthetic Arrhenius data (Figs 2–4 & 7), our attempts to graphically estimate the diffusion parameters for phengite consistently (and often substantially) underestimate the activation energy that is inferred using the inversion process. At the same time, our estimates for the parameters that applied to the model muscovite accurately reflect what can be graphically estimated. The modelling

Fig. 8. Inverse modelling allows inference of the diffusion parameters for the first part of the release spectrum. In (**a**) the muscovite domain activation energy (58.2 kcal/mol) appears to be accurately estimated, whereas the average slope in the steep zone on the Arrhenius plot gives an activation energy (121 kcal/mol), which is replicated in (**b**) but only if the maximum gradient in (a) is utilized, corresponding to a high activation energy of approximately 168 kcal/mol. Finally, the normalized frequency factor is iterated to allow correspondence with the muscovite release segment of the Arrhenius plot (**c**). The r/r_0 plots show an accurate correspondence between measured data (**d**) and that simulated using the *eArgon* program (**e**).

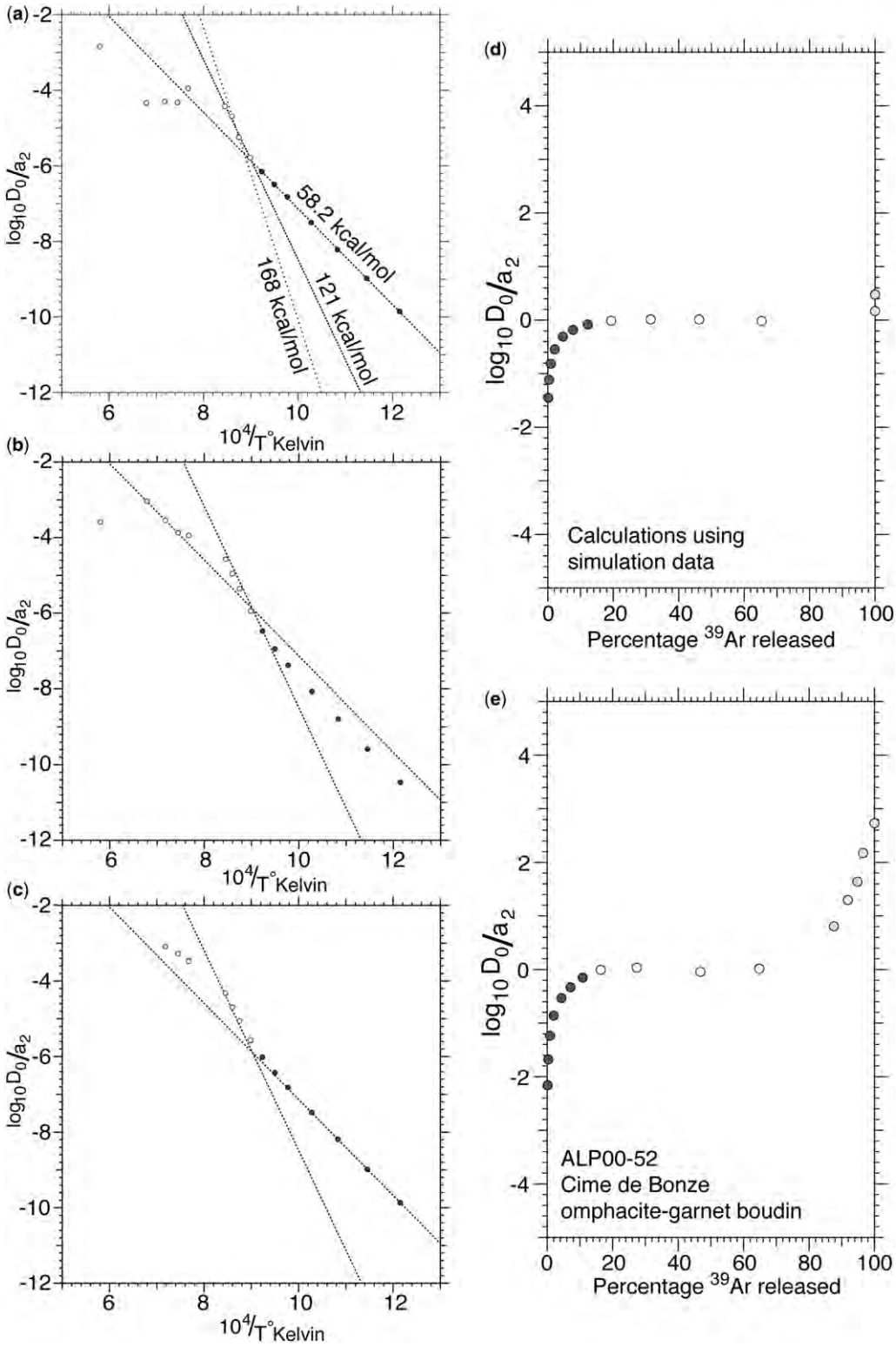

experiments seem to suggest that reliable estimates for the diffusion parameters can be obtained, but the question as to whether these are unique needs to be systematically addressed. Note also that the pattern of gas release from the two different reservoirs can be illustrated using a r/r_0 plot, although the mathematics used to make such plots is invalidated by the fact that different activation energies apply. Nevertheless, the pattern obtained in the r/r_0 plot is similar to that obtained using fractal size–volume distributions (Forster *et al.* 2011).

Pressure sensitivity of the diffusion parameters

The apparent age spectrum for the sample analysed above (ALP00-52) is shown in Figure 7. It is of interest that the initial sequence of steps produce age data that rise asymptotically (Forster & Lister 2004) towards a limit of about 69 Ma, which can be compared with a U–Pb age of 68 $\pm$ 7 Ma obtained by analysis of zircon rims by Liermann *et al.* (2002). Note, however, that Liermann *et al.* (2002) chose to ascribe this age to constrain the timing of early high-pressure metamorphism. The argon data suggest otherwise. The Arrhenius plot shows a change of slope, and the asymptotically rising steps correspond to steps that we infer to dominantly reflect the release of gas from the muscovite reservoirs. In this case what we estimate is the time at which exhumation of these metamorphic rocks took place, during which muscovite grains grew in the extensional shear zones responsible for their exhumation.

How is it possible for muscovite to retain argon at the temperatures that have been estimated to apply under such conditions (Beltrando *et al.* 2007; Rubatto *et al.* 2011), namely approximately 15–20 kbar and 550–600 °C.

The inversion of Arrhenius data recorded above takes no account of pressure, and neither is it able to account for this effect. Yet, the effect of pressure in respect to decreasing diffusivity is key to enabling forward modelling of the effect of temperature with time in the natural environment (Lister & Baldwin 1996; Warren *et al.* 2011). This is important and we do need to consider this effect when examining data from high-pressure terranes, as evident in our focus on phengite–muscovite mixtures, and in particular if we are to explain the approximately 69 Ma estimated age of the initial exhumation for the Cima de Bonze sample (Fig. 7). As noted above, this estimate is provided by the asymptotic rise in age recorded by steps in the heating sequence that we infer to have been dominated by the release of argon from muscovite.

Can pressure alone account for this retentivity?

Harrison *et al.* (2009) presented an analysis of experimental data for diffusion of argon in muscovite, for 10 and 20 kbar, but they made an error in the way that they calculated the activation volume. For experiments performed at 20 kbar, Harrison *et al.* (2009, p. 1047) wrote that 'Diffusion coefficients are reduced from their equivalent 10 kbar values by close to an order of magnitude which corresponds to an activation volume of 14 cm^3/mol'. This is not the value that can be calculated based on the Arrhenius equation so the data from the Harrison *et al.* (2009) experiments at 10 kbar (Table 3) were re-analysed. A regression was performed that yielded an activation energy of 62.5 kcal/mol (assuming spherical diffusion geometry) with a frequency factor of 2.33 $cm^2\ s^{-1}$, which values are as reported by Harrison *et al.* (2009). Using these data, the three experiments at 20 kbar could be re-analysed, this time using the Arrhenius equation (Table 4). This re-analysis yielded an average activation volume of 15.4 cm^3. This value in turn can be utilized to reduce the activation energy inferred for the 10 kbar data to zero pressure, yielding a value of 58.8 kcal/mol, which differs little from the 57.9 kcal/mol value reported by Giletti (1974). However, there are three experiments reported at 20 kbar, and one experiment yielded substantially different results to the other two. If the outlier is rejected, the estimate for the activation volume increases to 18 $\pm$ 0.6 cm^3.

Interestingly, this value for the activation volume is approximately 12.8% of the base multiple atomic volume used in defining allotropes for muscovite (e.g. $2M_1$, 1M, $1M_d$ or 3T: Deer *et al.* 2004) and, thus, of the same order as observed for other materials. Hence, while the paucity of available data limit the significance of any conclusions, it is interesting to consider the impact of this relatively high activation volume in modelling and simulation. Taking this value (i.e. 18 cm^3) for the activation volume also allows reduction of the 10 kbar data provided by Harrison *et al.* (2009). The results show that the zero pressure equivalent activation energy reduces to 58.2 kcal/mol. These are estimates that are within error of the value for the activation energy obtained for phlogopite, as provided by Giletti (1974) and Giletti & Tullis (1977), and the upper limit used by Lister & Baldwin (1996) in their simulations of the diffusion of argon in white mica.

The 10 kbar data reduced to zero pressure yielded modest closure temperatures (e.g. 371 °C for a 20 °C/Ma cooling rate). However, under high-pressure conditions there is a substantial increase (e.g. 417 °C for cooling at 20 °C/Ma at 10 kbar).

Table 3. *Data from Harrison et al. (2009) re-analysed in this paper to correctly estimate activation volume*

Temperature (°C)	Pressure (kbar)	log *D*	Temperature (K)	1000/K
730	10	−13.04	1003.15	0.99686
730	10	−12.92	1003.15	0.99686
730	10	−12.9	1003.15	0.99686
680	10	−13.82	953.15	1.04915
660	10	−14.23	933.15	1.07164
600	10	−15.15	873.15	1.14528
680	10	−13.6	953.15	1.04915
630	10	−14.83	903.15	1.10724
680	10	−13.86	953.15	1.04915
680	10	−14.35	953.15	1.04915
730	10	−13.63	1003.15	0.99686
730	10	−13.55	1003.15	0.99686
730	10	−13.42	1003.15	0.99686
730	10	−13.43	1003.15	0.99686
630	10	−15.05	903.15	1.10724
680	10	−13.75	953.15	1.04915
680	20	−14.98	953.15	1.04915
680	20	−14.53	953.15	1.04915
730	20	−14.15	1003.15	0.99686

Under ultra-high-pressure conditions the effect is even more marked (e.g. 464 °C for cooling at 20 °C/Ma at 20 kbar). For diamond facies conditions (e.g. 40 kbar), the closure temperature for cooling at 20 °C/Ma rises to 556 °C. Under such conditions muscovite could well retain relatively old apparent ages, and allow direct dating of the timing if its growth during exhumation is caused by the operation of extensional ductile shear zones.

For the one sample considered in detail (Fig. 7), inverting the Arrhenius data has provided us with an estimate of the diffusion parameters. Re-analysis of the Harrison *et al.* (2009) data has provided potentially high estimates for the activation volume. Hence, the next step was to forward model the effect of different pressure–temperature–time histories in order to ascertain the apparent age spectra that would result.

To do this we used the *MacArgon* program, now substantially modified from the version published by Lister & Baldwin (1996), but still essentially the same algorithm (although now in *C++* and *Objective C*). We imposed the same step-heating sequence in the MacSpectrometer as was used during the analysis of ALP00-52 in the ANU Argon Laboratory. We made no attempt to infer the actual variation of pressure and temperature with time in the natural environment for ALP00-52 was subjected to a complex evolution, the details of which are far beyond the scope of this paper. To properly constrain this history we require more data, in particular because we know that a complex multi-stage history was involved.

Here we simulate only the effects of simple cooling histories, with pressure decreasing linearly from 20 kbar during the period of high-pressure

Table 4. *Estimates for activation volume based on data reported by Harrison* et al. *(2009) from experiments at 20 kbar, and the recalculated zero pressure activation energy that is implied. The recalculated zero pressure activation energy is within the same error as that estimated by Giletti & Tullis (1977) for phlogopite*

Temperature (°C)	Pressure (kbar)	Activation energy at 20 kbar (kcal/mol)	Activation volume (cm^3)	Activation energy at 0 kbar (kcal/mol)
680	20	66.94	18.66	58.02
680	20	64.97	10.44	59.98
730	20	66.64	17.41	58.32

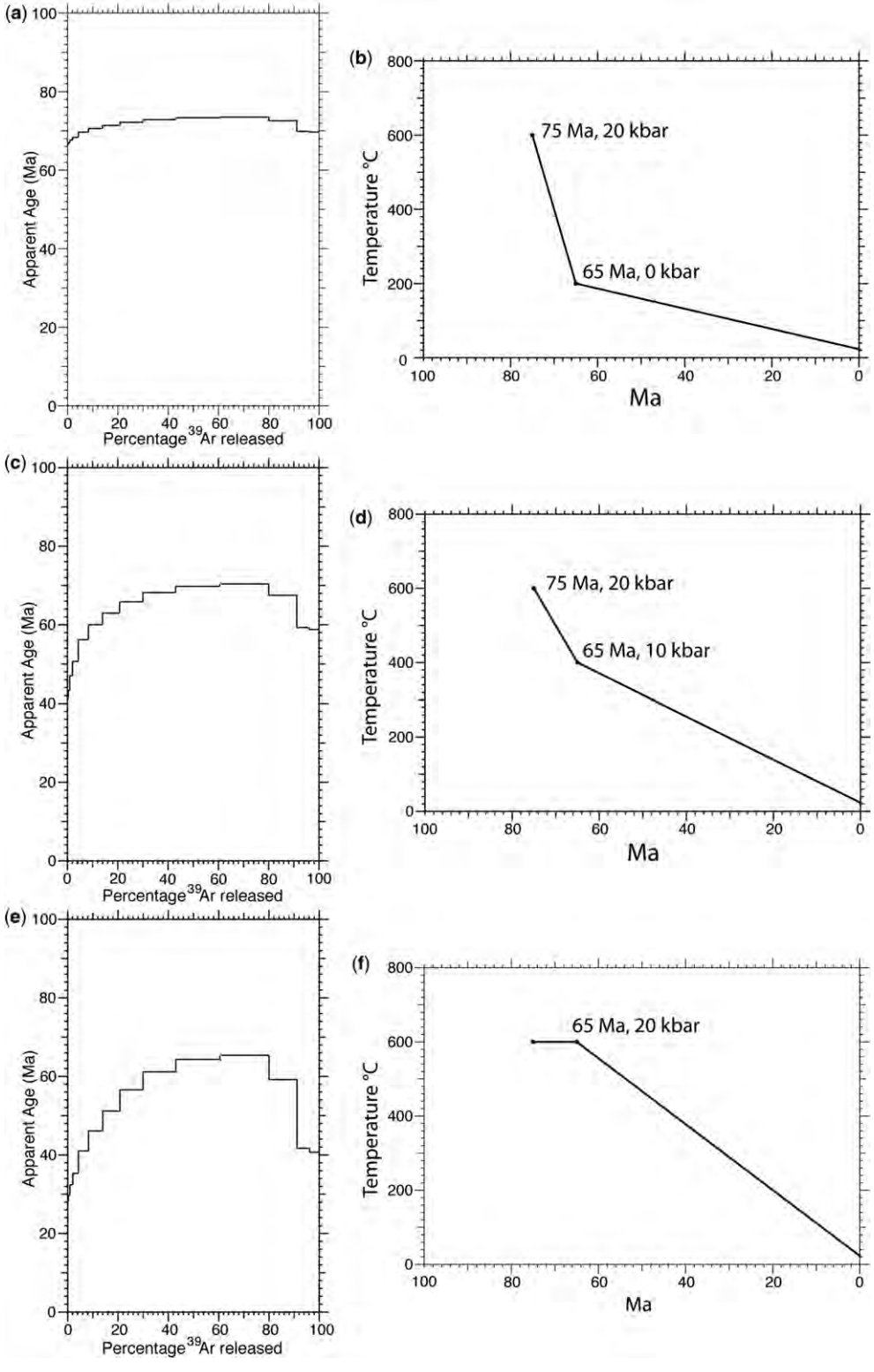

metamorphism to zero at the end of the cooling history. The 'hump-backed' apparent age spectra that result are reminiscent of those observed in such rocks, but the 'hump-backed' shape in the apparent age spectrum is less obvious in fast cooled samples (Fig. 9a) in comparison with those subject to slow cooling (Fig. 9c). In each case, the upwards-bounding limit underestimates the age of high-pressure metamorphism but not by a significant amount. These results thus support the possibility that $^{40}Ar/^{39}Ar$ geochronology may allow the direct dating of white mica mineral growth during metamorphism, supporting conclusions already reached by Mulch & Cosca (2004).

Discussion and conclusion

These are early days in respect of implementing a systematic approach to argon diffusion in white mica. The next steps require the collection of data, analysis and the correlation of estimated diffusion parameters with mineral chemistry. It is also appropriate that we attempt to analyse these data in terms of forward modelling the effects of pressure–temperature–time histories to which particular rocks may be have been subjected.

It is interesting that muscovite in the sample in question (ALP52-00) may record the age of its initial (partial) exhumation. The asymptotic rise of the apparent age to approximately 69 Ma is recorded in the first seven–eight heating steps, which are dominated by the release of ^{39}Ar from muscovite. This result suggests that systematic analysis of data from step-heating experiments may allow the timing of exhumation to be routinely estimated.

The asymptotic rise of ages obtained for the first part of the apparent age spectrum define a minimum age for the formation and/or cooling of the muscovite, at about 69 Ma. Interestingly, these steps on the Arrhenius plot define a linear alignment that predicts an activation energy of approximately 59 kcal/mol, which is comparable to the result obtained by Giletti & Tullis (1977) for phlogopite at room pressure or the pressure-corrected activation energy obtained by Harrison *et al.* (2009) on white mica heated and recrystallized at 10 kbar.

The age of prior high-pressure metamorphism may be somewhat older (*c.* 70–75 Ma) based on the scattered data from the steps dominated by the release of ^{39}Ar from phengite. The second part of the release spectrum is more haphazard, and suggests chaotic mixing between phengite and muscovite components. Nevertheless, these results lend support to the hypothesis that $^{40}Ar/^{39}Ar$ geochronology may, under certain conditions, directly date the timing of phengite growth (Putlitz *et al.* 2005). Overall, our simulations demonstrate that white mica in high-pressure terranes can be remarkably retentive.

One question asked of us by a reviewer was whether we could provide an explanation as to the widely differing activation energy obtained for phengite in comparison with other phyllosilicates, in particular given that these micas share the same basic lattice structure. We cannot explain why this is so, although we comment that activation energy alone does not determine retentivity of a mineral in respect to preventing argon loss. However, if we were to make an educated guess as to the direction that future research might take, it would be to suggest that we pay attention to *ab initio* calculations as reported by Huber *et al.* (2011) using a 3D Boltzmann model to simulate the effect of anisotropic diffusion. As temperatures increase, the pattern of vibrations in the lattice may allow diffusion to switch from a rate-determining step that fosters dominantly *c*-perpendicular diffusion (along the phyllosilicate sheets) to a rate-determining step that favours *c*-parallel diffusion (across the phyllosilicate sheets). This switch may be enhanced by variations in mineral chemistry as observed in phengite. Such a model is implicit in the assumption of a temperature-dependent (second-rank) 3D diffusion tensor. We have already noted that the simulations reported by Huber *et al.* (2011) produce gradual changes of slope that are reminiscent of some data as reported here.

It is also important to acknowledge the uncertainty that remains as to the changes in mineral structure that may take place on the atomic scale during step-heating experiments *in vacuo*. In addition, we should note that solid-state diffusion of argon is not of necessity a univariant phenomenon that depends solely on Boltzmann-type meanderings. Diffusion of argon may involve a rate-dependent step that is controlled by the mobility of other atoms (e.g. oxygen) and we should consider the possibility that argon moves with point

Fig. 9. The diffusion parameters inferred for sample ALP00-52 are used to simulate the development of apparent age spectra (**a**)–(**c**) with the *MacArgon* program. The step-heating sequence in the MacSpectrometer was set to imitate that used to measure sample ALP00-52. The activation volume utilized (18 cm^3) was calculated from diffusion data reported by Harrison *et al.* (2009). Considerable variation in the shape of the 'hump-backed' spectra result from these differing pressure–temperature–time paths but, in all cases, the phengite part of the release spectrum can be used to estimate a minimum age for high-pressure metamorphism.

defects related to the shuffling of different cations within the mineral structure. In this case, it should be expected that different mineral chemistries differ widely in their behaviour, including with respect to the diffusion of argon.

M. A. Forster acknowledges the support of an Australian Research Fellowship provided by the Australian Research Council (ARC). Research support was provided by ARC Discovery Grant DP0877274 'Tectonic mode switches and the nature of orogenesis'.

References

Baldwin, S. L. & Lister, G. S. 1998. Thermochronology of the South Cyclades Shear Zones, Ios, Greece: effects of ductile shear in the argon partial retention zone. *Journal of Geophysical Research*, **130**, 7315–7336.

Beltrando, M., Hermann, J., Lister, G. & Compagnoni, R. 2007. On the evolution of Orogens: pressure cycles and deformation mode switches. *Earth and Planetary Science Letters*, **256**, 372–388.

Cosca, M. A., Stunitz, H., Bourgeix, A.-L. & Lee, J. P. 2011. 40Ar* loss in experimentally deformed muscovite and biotite with implications for $^{40}Ar/^{39}Ar$ geochronology of naturally deformed rocks. *Geochimica et Cosmochimica Acta*, **75**, 7759–7778.

Crank, J. 1975. *The Mathematics of Diffusion*, 2nd edn. Oxford University Press, Oxford.

Deer, W. A., Howie, R. A., Zussman, J. & Fleet, M. E. 2004. *Rock Forming Minerals, Volume 3A: Micas*. Geological Society, London.

Forster, M. A. & Lister, G. S. 2004. The interpretation of $^{40}Ar/^{39}Ar$ apparent age spectra produced by mixing: application of the method of asymptotes and limits. *Journal of Structural Geology*, **26**, 287–305.

Forster, M. A. & Lister, G. S. 2010. Argon Enters the Retentive Zone: Reassessment of Diffusion Parameters for K-feldspar in the South Cyclades Shear Zone, Ios, Greece. *In*: Spalla, M. I., Marotta, A. M. & Gosso, G. (eds) *Advances in Interpretation of Geological Processes: Refinement of Multi-scale Data and Integration in Numerical Modelling*. Geological Society, London, Special Publications, **332**, 17–34, http://dx.doi.org/10.1144/SP332.2

Forster, M. A., White, L. T. & Ahmad, T. 2011. Thermal history of a pebble in the Indus Molasse at the margin of a Himalayan metamorphic core complex. *In*: Forster, M. A. & Fitz Gerald, J. D. (eds) *The Science of Microstructure – Part II*. *Journal of the Virtual Explorer*, **38**, paper 4, http://dx.doi.org/10.3809/jvirtex.2011.00267

Giletti, B. J. 1974. Studies in diffusion I: Argon in phlogopite mica. *In*: Hofmann, A. W., Giletti, B. J., Yoder, H. S. & Yund, R. A. (eds) *Geochemical Transport and Kinetics*. Carnegie Institution of Washington, Publications, **634**, 107–115.

Giletti, B. J. & Tullis, J. 1977. Studies in diffusion. IV. Pressure dependence of Ar diffusion in phlogopite mica. *Earth and Planetary Science Letters*, **35**, 180–183.

Hames, W. & Bowring, S. 1994. An empirical evaluation of the argon diffusion geometry in muscovite. *Earth and Planetary Science Letters*, **124**, 161–167.

Harrison, T. M., Cèlèrier, J., Aikman, A. B., Hermann, J. & Heizler, M. T. 2009. Diffusion of ^{40}Ar in muscovite. *Geochimica et Cosmochimica Acta*, **73**, 1039–1051.

Huber, C., Cassata, W. S. & Renne, P. R. 2011. A lattice Boltzmann model for noble gas diffusion in solids: the importance of domain shape and diffusive anisotropy and implications for thermochronometry. *Geochimica et Cosmochimica Acta*, **75**, 2170–2186.

Kirschner, D. L., Cosca, M. A., Masson, H. & Hunziker, J. C. 1996. Staircase $^{40}Ar/^{39}Ar$ spectra of fine-grained white mica: timing and duration of deformation and empirical constraints on argon diffusion. *Geology*, **24**, 747–750, http://dx.doi.org/10.1130/0091-7613(1996)024<0747:SAASOF>2.3.CO;2

Kula, J. & Spell, T. L. 2012. Recovery of muscovite age gradients by $^{40}Ar/^{39}Ar$ vacuum furnace step-heating analysis. *Chemical Geology*, **304–305**, 166–174, http://dx.doi.org/10.1016/j.chemgeo.2012.02.013

Kula, J., Spell, T. L. & Zanetti, K. A. 2010. $^{40}Ar/39Ar$ analyses of artificially mixed micas and the treatment of complex age spectra from samples with multiple mica populations. *Chemical Geology*, **275**, 67–77.

Liermann, H., Isachsen, C., Altenberger, U. & Oberhänsli, R. 2002. Behavior of zircon during high-pressure, low-temperature metamorphism: case study from the Internal Unit of the Sesia Zone (Western Italian Alps). *European Journal of Mineralogy*, **14**, 61–71.

Lister, G. S. & Baldwin, S. L. 1996. Modelling the effect of arbitrary P-T-t histories on argon diffusion in minerals using the MacArgon program for the Apple Macintosh. *Tectonophysics*, **253**, 83–109.

Lister, G. S. & Raouzaios, A. 1996. The tectonic significance of a porphyroblastic blueschist facies overprint during Alpine orogenesis: Sifnos, Aegean Sea, Greece. *Journal of Structural Geology*, **18**, 1417–1435.

Lovera, O. M., Grove, M., Harrison, T. M. & Mahon, K. I. 1997. Systematic analysis of K-feldspar $^{40}Ar/^{39}Ar$ step heating results: I. Significance of activation energy determinations. *Geochimica et Cosmochimica Acta*, **61**, 3171–3192.

Lovera, O. M., Grove, M. & Harrison, T. M. 2002. Systematic analysis of K-feldspar $^{40}Ar/^{39}Ar$ step heating results II: relevance of laboratory argon diffusion properties to nature. *Geochimica et Cosmochimica Acta*, **66**, 1237–1255.

McDougall, I. & Harrison, T. M. 1999. *Geochronology and Thermochronology by the $^{40}Ar/^{39}Ar$ Method*. Oxford University Press, Oxford.

Mulch, A. & Cosca, M. A. 2004. Recrystallization or cooling ages: in situ UV-laser $^{40}Ar/^{39}Ar$ geochronology of muscovite in mylonitic rocks. *Journal of the Geological Society*, **161**, 573–582.

Mulch, A., Cosca, M. A., Andresen, A. & Fiebig, J. 2005. Time scales of deformation and exhumation in extensional detachment systems determined by high-spatial resolution *in situ* UV-laser Ar/Ar dating. *Earth and Planetary Science Letters*, **233**, 375–390.

Putlitz, B., Cosca, M. A. & Schumacher, J. 2005. Prograde mica $^{40}Ar/^{39}Ar$ growth ages recorded in high

pressure rocks (Syros, Cyclades, Greece). *Chemical Geology*, **214**, 79–98.

Rubatto, D. R., Hermann, J., Boston, K., Engi, M., Beltrando, M. & Mcalpine, S. R. B. 2011. Yo/Yo subduction recorded by accessory minerals in the Italian Western Alps. *Nature Geoscience*, **4**, 338–342, http://dx.doi.org/10.1038/ngeo1124

Sherlock, S. C. & Arnaud, N. O. 1999. Flat plateau and impossible isochrons: apparent $^{40}Ar/^{39}Ar$ geochronology in a high-pressure terrain. *Geochimica et Cosmochimica Acta*, **63**, 2835–2838.

Sherlock, S., Kelley, S. P., Inger, S., Harris, N. & Okay, A. 1999. $^{40}Ar–^{39}Ar$ and Rb–Sr geochronology of high-pressure metamorphism and exhumation history of the Tavsanli Zone, NW Turkey. *Contributions to Mineralogy and Petrology*, **137**, 46–58.

Sletten, V. & Onstott, T. C. 1998. The effect of the instability of muscovite during *in vacuo* heating on $^{40}Ar/^{39}Ar$ step-heating spectra. *Geochimica et Cosmochimica Acta*, **62**, 123–141.

Viete, D. R., Forster, M. A. & Lister, G. S. 2011. The nature and origin of the Barrovian metamorphism, Scotland: $^{40}Ar/^{39}Ar$ apparent age patterns and the duration of metamorphism in the biotite zone. *Journal of the Geological Society*, **168**, 133–146, http://dx.doi.org/10.1144/0016-76492009-164

Warren, C. J., Hanke, F. & Kelley, S. P. 2011. When can muscovite $^{40}Ar/^{39}Ar$ dating constrain the timing of metamorphic exhumation? *Chemical Geology*, **291**, 79–86.

Watson, E. B., Wanser, K. & Farley, K. 2010. Anisotropic diffusion in a finite cylinder, with geochemical applications. *Geochimica et Cosmochimica Acta*, **74**, 614–633.

Wijbrans, J. R. & McDougall, I. 1986. $^{40}Ar/^{39}Ar$ dating of white micas from an Alpine high-pressure metamorphic belt on Naxos (Greece): the resetting of the argon isotopic system. *Contributions to Mineralogy and Petrology*, **93**, 187–194.

Wijbrans, J. R. & McDougall, I. 1988. Metamorphic evolution of the Attic Cycladic metamorphic belt on Naxos (Cyclades, Greece) utilizing $^{40}Ar/^{39}Ar$ age spectrum measurements. *Journal of Metamorphic Geology*, **6**, 571–594.